Nonlocal Problems in MEMS Device Control

J.A. Pelesko* and A.A. Triolo**

*Georgia Institute of Technology, School of Mathematics
Atlanta, GA, USA, pelesko@math.gatech.edu
**Lucent Technologies, Wireless Technology Laboratory
Whippany, NJ, USA, atriolo@lucent.com

ABSTRACT

Perhaps the most ubiquitous phenomena associated with electrostatically actuated MEMS devices is the "pull-in" voltage instability. In this instability, when applied voltages are increased beyond a certain critical voltage there is no longer a steady-state configuration of the device where mechanical members remain separate. This instability severely restricts the range of stable operation of many devices. Here, a mathematical model of an idealized electrostatically actuated MEMS device is constructed for the purpose of analyzing various schemes proposed for the control of the pull-in instability. This embedding of a device into a control circuit gives rise to a nonlinear and nonlocal elliptic problem which is analyzed through a variety of asymptotic, analytical, and numerical techniques. Variations in capacitive control schemes are shown to give rise to variations in solutions of the model and hence to effect the pull-in voltage and pull-in distance.

Keywords: MEMS control, electrostatic actuation, pull-in, instability, nonlocal elliptic problem

1 INTRODUCTION

The pull-in voltage instability is a seemingly universal phenomena in the world of electrostatically actuated MEMS devices. Even as early as 1967, MEMS pioneers such as Nathanson, [1], were aware that when applied voltages are increased beyond a certain critical voltage there is no longer a steady-state configuration of many electrostatically actuated devices where mechanical members remain separate.

Recently, several authors have proposed and analyzed control schemes in an effort to overcome this instability. Chu and Pister, [2], proposed a voltage control algorithm, while Seeger and Crary, [3], [4], and Chan and Dutton, [5], studied capacitive control schemes. In this paper we focus on control via the addition of a series capacitance. In [3], Seeger and Crary analyzed this scheme with the use of a mass-spring model. In the course of their analysis, nonlinear terms arising from the electrostatic force and from the additional capacitance were found to cancel. This led to the result that the scheme could stabilize a device over the entire range of motion. In [5], 2-d effects were included in a mass-spring model through the addition of parasitic capacitance's to the circuit. Mathematically, this removed the cancellation of nonlinear terms seen by Seeger and Crary and led to the conjecture that the control scheme is only partially stabilizing.

In this paper, we analyze the fixed capacitance control scheme in the context of a two dimensional model. In particular, we model the device shown in Figure 1, which consists of an elastic strip suspended above a rigid plate. The device is assumed to be connected in series in a closed circuit with a fixed voltage source, V_s, and a fixed capacitor. The model then consists of the circuit equations, the equation of elasticity for the strip, and the potential equation for the electrostatic field. A summary of the analysis of this model is presented below. The detailed analysis, including a discussion of varactor based control schemes is given in [6].

2 THE MATHEMATICAL MODEL

In this section we present the governing equations for the behavior of an idealized electrostatically actuated MEMS device. The geometry of the device is sketched in Figure 1. We embed the device in a control circuit,

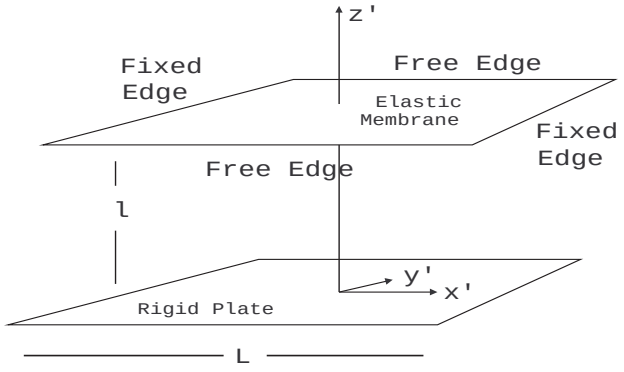

Figure 1: Geometry of our idealized MEMS device

that is, we assume that the device is placed in series in a closed circuit with a battery and a fixed capacitor.

The electrostatic potential satisfies Laplace's equation everywhere away from the two plates, and appropriate boundary conditions on the plates. In dimensionless form these equations may be written as

$$\epsilon^2(\frac{\partial^2\psi}{\partial x^2} + a^2\frac{\partial^2\psi}{\partial y^2}) + \frac{\partial^2\psi}{\partial z^2} = 0, \tag{1}$$

$$\psi(x,y,-1) = 0 \quad x \in [-1/2,1/2] \quad y \in [-1/2,1/2] \tag{2}$$

$$\psi(x,y,u) = f(u) \quad x \in [-1/2,1/2] \quad y \in [-1/2,1/2] \tag{3}$$

where here, ψ is a dimensionless potential scaled with respect to the source voltage, x and y are scaled with respect to the length and width of the undeformed plate, ϵ is an aspect ratio of the device comparing device length to undeformed gap size, a is the aspect ratio of the device itself and u is the displacement of the top plate scaled with respect to undeformed gap size. The function $f(u)$ reflects the fact that when embedded in a circuit the voltage drop across the device depends upon the deflection. Note that we are assuming that u is a function of x alone. This displacement is assumed to satisfy

$$\frac{d^2u}{dx^2} = \beta\left(\epsilon^2(\frac{\partial\psi}{\partial x})^2 + \epsilon^2a^2(\frac{\partial\psi}{\partial y})^2 + (\frac{\partial\psi}{\partial z})^2\right) \tag{4}$$

$$u(-1/2) = u(1/2) = 0. \tag{5}$$

Here, $\beta = \epsilon_0V_s^2L^2/2Tl^3$, where l is undeflected gap size, L is length of the plate, T is tension, and ϵ_0 is the permittivity of free space. Note that β characterizes the relative strengths of electrostatic and mechanical forces in the problem. We are assuming that the top plate is held fixed along the edges at $x = \pm 1/2$ and is free along the remaining edges. Finally, Kirchoff's laws may be applied to the circuit to find the voltage drop across our device. In dimensionless form, this is precisley $f(u)$, and we find

$$f(u) = \frac{1}{1 + C/C_f}. \tag{6}$$

Here, C_f is the capacitance of the fixed capacitor, while C is the capacitance of the device itself. Note that C is not constant, but rather depends upon u.

Next, we simplify our governing equations by assuming that the aspect ratio, ϵ, is small. Accordingly, we send ϵ to zero, solve the resulting simplified potential equation and use this approximate potential in the elastic equation. Similiarly we can use the same asymptotic approximation to compute C. The upshot of this analysis is that the problem can be reduced to the following nonlocal elliptic equation for the displacement

$$\frac{d^2u}{dx^2} = \frac{\beta}{(1+u)^2(1+\chi\int_{-1/2}^{1/2}\frac{d\zeta}{1+u(\zeta)})^2} \tag{7}$$

with the boundary conditions given by equation (5). Here, χ, is a ratio of the capacitance of our undeflected device to the capacitance of the fixed capacitor in the circuit. Throughout the remainder of this paper we shall analyze the solutions of the reduced model, equations (5) and (7), in order to understand the circuits influence on our MEMS device.

3 ANALYSIS OF REDUCED MODEL

A few elementary properties of solutions to equations (5) and (7) follow almost by inspection. First, we see that the equation is invariant under the transformation $x \to -x$ and hence solutions are symmetric, i.e., $u(x) = u(-x)$. Second, since the second derivative is everywhere positive for positive β, the solution must be concave up everywhere or more succinctly, convex. Combining the convexity result with the symmetry result implies that $u(x) \geq u(0)$ for all $x \in [-1/2,1/2]$. Finally, since the solution must be zero on the boundaries, and remain convex, we have that $u(x) \leq 0$ for all $x \in [-1/2,1/2]$ as well.

Next, we observe that equation (7) is *nonlocal*. In order to obtain a detailed understanding of this nonlocal problem, which we denote (NLP), we will need to understand the nature of solutions for the associated local problem denoted (LP) and defined by

$$\frac{d^2u}{dx^2} = \frac{\lambda}{(1+u)^2} \tag{8}$$

$$u(-1/2) = u(1/2) = 0. \tag{9}$$

We note that this system of equations governs the deflection of the membrane when the only other circuit element is a fixed voltage source. This may be seen as the problem (LP) results from setting $\chi = 0$ in (NLP). The relationship between solutions of problem (NLP) and problem (LP) is captured by the following observation:

Observation - A solution, u, of problem (NLP) is a solution of problem (LP) for $\lambda = \frac{\beta}{(1+\chi\int_{-1/2}^{1/2}\frac{d\zeta}{1+u(\zeta)})^2}$ while a solution, u, of problem (LP) is a solution of problem (NLP) for $\beta = \lambda(1+\chi\int_{-1/2}^{1/2}\frac{d\zeta}{1+u(\zeta)})^2$.

Note that this implies that the set of solutions to (LP) and (NLP) are identical. Hence results concerning (LP) may be translated into results for (NLP), the translation being through the mapping between β and λ given above. We further note that (LP) was analyzed extensivley in [7] and in fact the results mentioned above for (NLP) could have been proved by comparison with (LP) together with our observation.

The relationship between (NLP) and (LP) is particularly usefull when we wish to sketch the bifurcation diagram for (NLP). In [7] the following implicit formulas for the solution of problem (LP) were derived

$$\sqrt{\frac{(u+1)(u+1-\lambda/E)}{2E}} + \tag{10}$$

$$\frac{\lambda}{E\sqrt{2E}}\tanh^{-1}\sqrt{\frac{u+1-\beta/E}{u+1}} = x$$

$$\sqrt{\frac{1-\lambda/E}{2E}} + \frac{\lambda}{E\sqrt{2E}}\tanh^{-1}\sqrt{1-\lambda/E} = \frac{1}{2}. \quad (11)$$

By numerically solving equation (11) for E as a function of λ, using this result in equation (11) to compute $u(x,\lambda)$, and combining with the mapping between (LP) and (NLP), we may sketch the bifurcation diagram for problem (NLP). This is done in Figure 2 for various values of χ.

At this point, the analysis of the capacitive control scheme for our device is essentially complete. However, the reliance on the exact solution to (LP) in order to establish the pull-in property and sketch the bifurcation diagram for (NLP) is somewhat unsatisfying. In particular, if we wished to change from our "strip" geometry to an arbitrarily shaped device, we cannot expect to have an exact solution to the local problem available. With this in mind, a few results are presented in [6] which begin to generalize our analysis from the strip geometry to an arbitrarily shaped device. We establish the fact that the pull-in property is a generic feature of a generalized local problem (GLP). That is, we show that the pull-in phenomena occurs for a MEMS device of rather arbitrary geometry. To establish that when embedded in the capacitive control scheme, an arbitratily shaped device still possesses the pull-in property would require a detail study of the mapping between (LP) and (NLP) for all possible shapes. We do not carry out such an analysis. Rather, for our strip problem we outline a methodology that allows one to determine if the controlled device still has the pull-in property, even when an exact solution to the local problem is unavailable. Hence, we expect this methodology to be usefull in the study of arbitrarily shaped devices.

The essential question is whether or not the curve of solutions in the bifurcation diagram "bends back" upon itself. From the exact solution we know that it does for (LP). Now, we must determine how this folded curve maps into the bifurcation diagram for (NLP) under the mapping in our observation. We introduce the initial value problem (IVP)

$$\frac{d^2w}{dx^2} = \frac{1}{w^2} \quad (12)$$

$$w(0) = 1 \quad w'(0) = 0. \quad (13)$$

If we let $c = -u(0)$ then all solutions to (LP) can be generated from this initial value problem by setting $u(x) = aw(bx) - 1$ and then requiring that $a = \frac{1}{w(b/2)}$, $1 - c = a$ and $\frac{\lambda}{a^3b^2} = 1$. We may solve for λ in terms of b and w to find that $\lambda = \frac{b^2}{w(b/2)^3}$. We see that the behavior of the bifurcation curve for (LP) may be obtained by studying solutions of (IVP) for $x \to \infty$! The asymptotic behavior of solutions to (IVP) for arbitrary initial conditions was presented in [7]. It was shown that

$$w(x) \sim \alpha x - \frac{1}{\alpha^2}\log(x) + \cdots \quad (14)$$

Combining this with our expression for λ, we find that $\lambda \sim \frac{1}{\alpha b}$ as $b \to \infty$. Hence the bifurcation curve for (LP) bends back and approaches $\lambda = 0$. Finally, we may substitute our expressions for λ and u into our mapping in our observation. We find that

$$\beta = \frac{b^2}{w(b/2)^3}(1 + \chi\frac{w(b/2)}{b}\int_{-b/2}^{b/2}\frac{dy}{w(y)})^2. \quad (15)$$

Now, from our asymptotic approximation for w, we see that the first term in this expression goes like $1/b$ as $b \to \infty$ while the term in parentheses goes no faster than $\log(b)$. Hence the bifurcation curve for (NLP) also bends back and approaches $\beta = 0$.

4 DISCUSSION

We began by formulating a model of an idealized electrostatically actuated MEMS device embedded in a control circuit. The model consisted of three parts. First, the electrostatic potential on and around the device was assumed to satisfy Laplace's equation with the appropriate boundary conditions. Second, the elastic displacement of the device was assumed to satisfy an elliptic ordinary differential equation. The model geometry, a rectangular elastic membrane suspended above a rigid plate, together with assumptions concerning the elastic boundary conditions allowed us to make the assumption that the elastic displacement, u, was a function of a single spatial variable. We note that the electrostatic and elastic problems were coupled nonlinearly. That is, the location of the boundary conditions for the electrostatic problem depended upon the elastic displacement, while the forcing term in the elastic equation was proportional to the norm of the gradient of the potential, squared. The third part of the model consisted of equations governing the behavior of the circuit in which our MEMS device was embedded. These equations were derived by applying Kirchoff's laws. We note that the circuit equations were coupled to both the electrostatic and elastic problems. In particular, the potential drop specified in the electrostatic boundary conditions depended upon circuit behavior, while the circuit behavior depended upon the capacitance of the MEMS device and hence depended upon the elastic displacement, u.

Our next step was to simplify the model. Our main approximation was to use the small aspect ratio of our MEMS device to obtain an approximate solution to the

potential equation. Simply put, we ignored fringing fields. The accuracy of this approximation was investigated by comparing the approximate solution to numerically obtained exact solutions. The upshot of this comparison is that for small aspect ratios, the approximate potential is very close to the exact. The reader is referred to [6] for details of this numerical study. With this approximate solution in hand, we next turned to the elastic and circuit equations.

The reduced model, i.e. using the approximate potential, was studied for a proposed control circuit. In order to see the effect of the control circuit it is useful to examine the behavior of our MEMS device when it is placed in a closed circuit with a fixed voltage source. We note that this corresponds to setting $\chi = 0$ in problem (NLP) from Section 3. The bifurcation diagram for positive values of β is sketched in Figure 2 and corresponds to the $\chi = 0$ curve. We see that the bifurcation diagram consists of a single fold and hence for positive values of β less than some critical value β^*, two solutions exist. As β approaches β^* these solutions collide and at β^* they disappear. This critical value β^* corresponds to the pull-in voltage and hence we have characterized the pull-in instability in terms of this bifurcation diagram. That is, for $\beta > \beta^*$, no steady-state solution of the problem exists, i.e. the elastic membrane has collapsed onto the rigid plate. We further note that the pull-in distance corresponds to the value of $||u||$ at $\beta = \beta^*$.

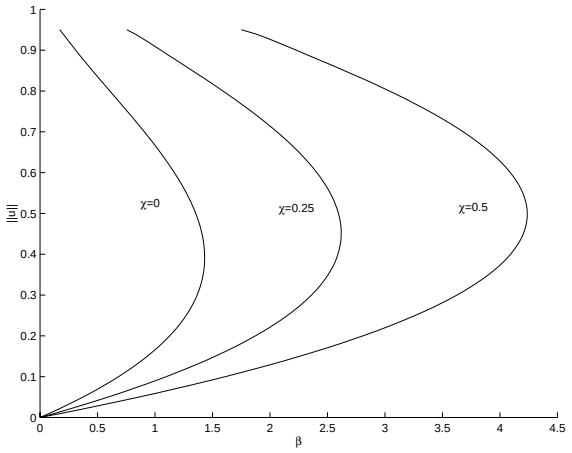

Figure 2: Maximum displacement vs. β

Now, we can use our model to examine the effect of a control circuit on the stability of our MEMS device. We turn our attention to the simple fixed capacitive control scheme proposed by Seeger and Crary in [3]. Seeger and Crary studied this scheme by using a simple mass-spring model to model the elastic behavior of a MEMS device. Further they concluded that the fixed capacitive control scheme fully stabilized the device, effectively removing the pull-in instability. At odds with this conclusion was the result obtained by Chan and Dutton in [5]. Chan and Dutton, like Seeger and Crary, used a mass-spring model, but they began to include two dimensional effects by adding parasitic capacitance's to the circuit. On the basis of this model they concluded that pull-in persists. By plotting the bifurcation diagram for the fixed capacitive control model studied in Section 3, we also conclude that pull-in persists. Again turning to Figure 2 and this time focusing on curves for $\chi > 0$, we see that the bifurcation diagram for this system is still characterized in terms of a single fold. Again, this implies that for β greater than some critical value β^*, no steady solutions exist and pull-in has occurred. We also note that as χ is increased, the "nose" of the curve moves up and to the right. This implies that the fixed capacitive scheme is partially stabilizing. That is, the achievable maximum displacement has increased. Again examining Figure 2, we see that this stabilization comes at a price, higher voltages are needed to obtain a given displacement.

Finally, we again refer the interested reader to [6] where details of the analysis are given, the varactor or MOS capacitor control scheme is analyzed, and some further generalizations are discussed.

REFERENCES

[1] H.C. Nathanson, W.E. Newell, R.A. Wickstrom and J.R. Davis, "The Resonant Gate Transistor", IEEE Trans. on Electron Devices, 14 (1967), pp. 117-133.

[2] P.B. Chu and K.S.J. Pister, "Analysis of Closed-loop Control of Parallel-Plate Electrostatic Microgrippers", Proc. IEEE Int. Conf. Robotics and Automation, (1994), pp. 820-825.

[3] J.I. Seeger and S.B. Crary, "Stabilization of Electrostatically Acutated Mechanical Devices", Proc. of the 1997 Intl. Conf. on Solid-State Sensors and Actuators (1997), pp. 1133-1136.

[4] J.J. Seeger and S.B. Crary, "Analysis and Simulation of MOS Capacitor Feedback for Stabilizing Electrostatically Actuated Mechanical Devices", Second Int. Conf. on the Simulation and Design of Microsystems and Microstructures - MICROSIM97, (1997), pp. 199-208.

[5] E.K. Chan and R.W. Dutton, "Effects of Capacitors, Resistors and Residual Change on the Static and Dynamic Performance of Electrostatically Actuated Devices", Proc. of SPIE, 3680 (1999), pp. 120-130.

[6] J.A. Pelesko and A.A. Triolo, "Nonlocal Problems in MEMS Device Control", Jrnl. of Eng. Math., submitted.

[7] D. Bernstein, P. Guidotti and J.A. Pelesko, "Analytical and Numerical Analysis of Electrostatically Actuated MEMS Devices", Sensors and Actuators, submitted.